Iranian Journal of Chemical Engineering
Vol. 2, No. 2, 2005, IAChE

CFD Simulations of Pressure Drop in KATAPAK-S Structured Packing

M. Zivdar[*1] R. Rahimi[1], M. Nasr[2], M. Haghshenasfard[1]*
1. Department of Chemical Engineering, University of Sistan Baluchestan, Zahedan, 98164, Iran.
2. Department of Chemical Engineering, Isfahan University of Technology, Isfahan, 84156, Iran.

Abstract
KATAPAK-S is a type of structured catalytic packing, which is used in reactive distillation processes. The dry pressure drop characteristic (the pressure drop in the absence of liquid flow) is of significant importance for the investigation of process hydrodynamics. In this paper, the dry pressure drop within the catalyst packed channels of KATAPAK-S has been investigated using Computational Fluid Dynamics (CFD).
Results of the CFD simulations were validated using experimental pressure drop data and empirical correlations. The CFD results showed an excellent agreement with theoretical and experimental data.

Keywords: *KATAPAK-S structures, Pressure drop, Structured packing, CFD*

Introduction
Catalytic distillation is a process in which coupling of separation and chemical reaction occurs. This process is enjoying a lot of attention from industries and academia because of the many advantage over the conventional reaction followed by separation concept. The advantages of this process are: environmental protection, reduction of investment cost and lower energy consumption [1].
Some structured catalytic column internals have been developed in recent years such as KATAPAK-S (Figure 1), which is being licensed by Sulzer. This packing has a sandwich structure composed of corrugated sheets of wire gauze, made of stainless steel.
Catalyst particles are sandwiched between two corrugated sheets, joined together and placed in the column. The size of the catalyst pellets is 1 mm. A schematic view of these sheets is shown in Figure 2 [3].

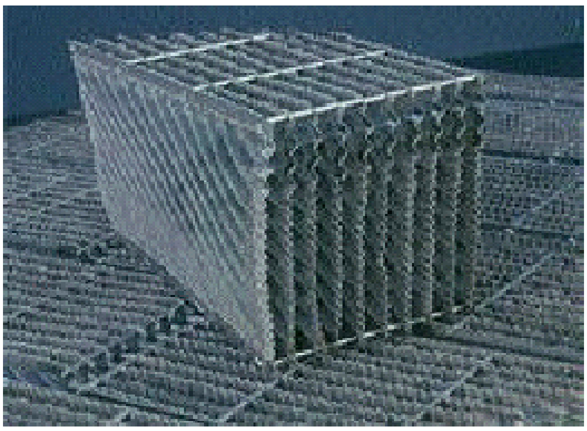

Figure 1. KATAPAK-S [1]

Krishna and co-workers have studied some of the important parameters such as mass

∗ - Corresponding Author: Email: mortaza@hamoon.usb.ac.ir

transfer coefficients and liquid phase dispersion in the KATAPAK-S structures [3-6]. The dry pressure drop characteristic is important for the investigation of process hydrodynamics and it is often the preliminary diagnostic tool for characterizing structured packings [7]. The use of CFD for design studies reduces the number of necessary experiments and yields results which would hardly be accessible by measurements, such as the pressure distribution in packed columns.

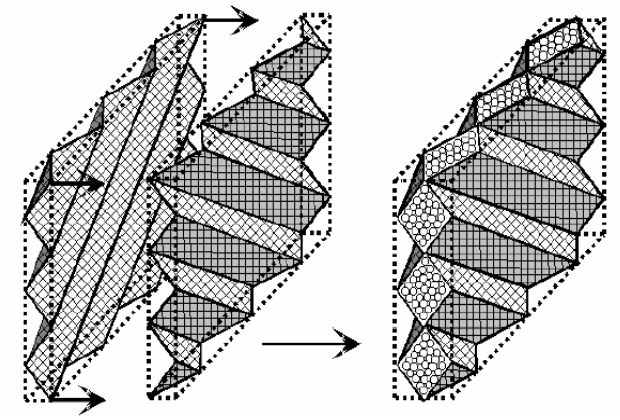

Figure 2. Schematic view of the KATAPAK-S sheet [3]

In this paper, a CFD analysis of dry pressure drop in corrugated sheet packings of KATAPAK-S is presented.

Theoretical Model

Petre and co-workers have investigated dry pressure drop for some types of the structured packings such as Mellapak, Gempak and Montzpak [8-9].

According to their model, the total pressure drop of a structured packing consists of four distinct contributions:

$$\Delta P_{tot} = \Delta P^{i} + \Delta p^{ii} + \Delta P^{iii} + \Delta P^{iv} \qquad (1)$$

In which:

ΔP^{i} = Elbow loss in bed entrance region.

ΔP^{ii} = Collision between two incoming gas jets meeting at criss-crossing junctions, ΔP^{iii} = Elbow loss at middle layers.

ΔP^{iv} = Pressure drop caused by the wall effects.

In this paper, a KATAPAK sheet with 16 triangular channels has been investigated, so the total pressure drop of the packed column is:

$$(\Delta P)_{total} = (\Delta P)_{Sheets} + (\Delta P)_{Elbow-entrance} + (\Delta P)_{Elbow-middle} \qquad (2)$$

In which:

$(\Delta P)_{sheets}$ = Static pressure gradient of the bed assembly of corrugated sheets catalytic packings. Wall effects have also been included in this parameter.

$(\Delta P)_{Elbow-entrance}$ = Pressure drop of the elbow in bed entrance region at the first layer.

$(\Delta P)_{Elbow-middle}$ = Pressure drop of the elbow at middle layers.

The locations of the sheet and elbow are shown in Figure 3.

The KATAPAK-S is modeled as a porous body with a friction factor Ψ. The dry pressure drop can be calculated from the Darcy-Weisbach equation:

$$\left(\frac{\Delta P}{H}\right)_{dry} = \Psi * \left(\frac{\rho_g U_g}{2d_h}\right) \qquad (3)$$

Ψ is the friction factor and is assumed to be a power function of the gas phase Reynolds number [10].

U_g is the effective gas velocity computed from the superficial gas velocity as [1]:

$$U_g = \frac{V}{\varepsilon} \tag{4}$$

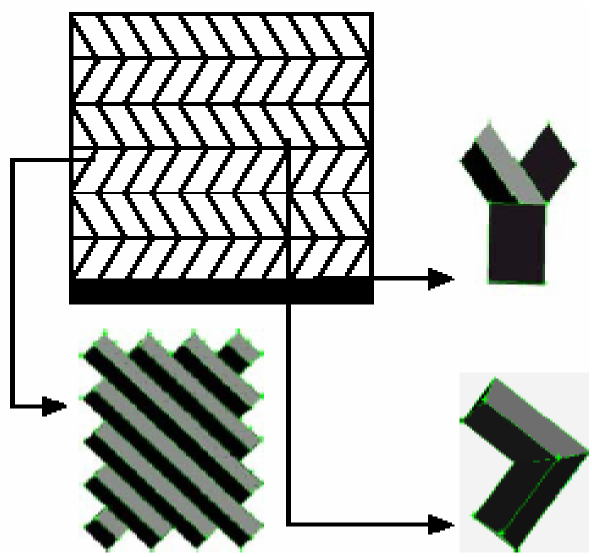

Figure 3. Location of the sheet and elbows

According to Kolodziej and co-workers [1] d_h is the hydraulic packing diameter and K is the wall factor.

$$d_h = \frac{4\varepsilon K}{a_p}\ ,\ K = 1/\left(1 + 4/a_p D\right) \tag{5}$$

Substituting Eqs. 4 and 5 in Eq. 3 results in:

$$\left(\frac{\Delta P}{H}\right)_{dry} = \Psi * \left(\frac{\rho_g . V^2 . a_p}{8\varepsilon^3 K}\right) \tag{6}$$

The friction factor Ψ can be calculated from empirical correlations [1]:

$$\Psi = 6.275 * \mathrm{Re}^{-0.293} \quad \text{For } 550 < \mathrm{Re} < 1550 \tag{7}$$

$$\Psi = 2.561 * \mathrm{Re}^{-0.171} \quad \text{For } 1550 < \mathrm{Re} < 6000 \tag{8}$$

Gas phase Reynold number is defined by:

$$\mathrm{Re} = \frac{\rho_g . V . d_h}{\mu_g} \tag{9}$$

The results of the above model have been compared with CFD simulation results and experimental data.

CFD Modeling

The 3-D computational domains for the CFD simulation of gas flow in a single sandwich structure of KATAPAK and in the elbow at the first layer are shown in Figure 4.

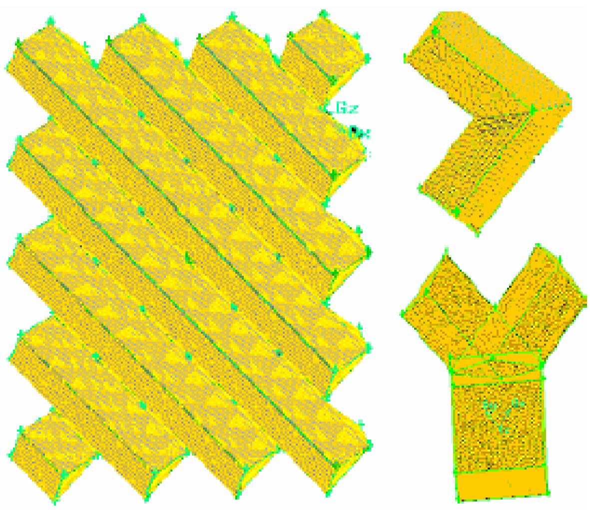

Figure 4. Computational domain

The sandwich consists of 16 triangular channels with a total of 32 cross-overs [2]. Geometrical and surface characteristics of the KATAPAK are shown in table 1. The general conservation equations describing the gas flow taking place within KATAPAK consist of the continuity and the Navier-Stokes equations. As mentioned above, the KATA-PAK-S is modeled as a porous body. For transient porous media calculations, the effect of porosity on the time-derivative terms is accounted for in all scalar transport equations and the continuity equation. When the effect of porosity is accounted for, the time-derivative term becomes $\frac{\partial}{\partial t}(\varepsilon\rho\Phi)$, where Φ is the scalar quantity and ε is the porosity. The continuity and momentum equations for the gas phase are:

$$\frac{\partial \varepsilon \rho_g}{\partial t} + \nabla.(\rho_g.\varepsilon.V) = 0 \quad (10)$$

$$\frac{\partial \varepsilon \rho_g.V}{\partial t} + \nabla.(\rho_g.\varepsilon.V.V - \mu_g \varepsilon(\nabla V + (\nabla V)^T)) = \varepsilon B - \varepsilon \nabla P \quad (11)$$

The gas phase was taken to be air with $\rho_g = 1.225(kg/m^3), \mu = 1.7894e-5(kg/m.s)$ and the porosity of the system is 0.622 m^3/m^3.

In the above equations, B is the body force resulting from the flow resistance [2]. The fluid flow is assumed isothermal and isotropic.

For solving the above equations, a commercial CFD package, Fluent 6, was used and mesh preparations were made in Gambit 2.0.4 For KATAPAK sheet and elbow, unstructured grids were generated. For this work, a PC 2.66 GHZ with 1024 Mb RAM was used.

For the gas phase, the low Reynolds $K-\varepsilon$ model was used. Each sheet includes eight inlets and eight outlets. At each inlet and at the elbow inlet, a specified velocity boundary condition is used and for each outlet, an “outflow” boundary condition is used.

At the sheet walls, the “wall boundary condition”, the non-slip condition is used.

Simulation Results and Discussion

The gas flow across the sheet and elbows is first simulated to compute the dry pressure drop. The gas flow passes through the entrance elbow and distributes between the sheets.

Contours of static pressure are used to predict the pressure drop and flow path lines plot. These can be used to illustrate the flow pattern, vortices and dead zones.

The 3-D gas flow path lines in the sheet and elbows are shown in Figure 5. From this figure, the path lines illustrate the complexity of the three-dimensional flow developed in the sheet. The path lines in the sheet are colored according to the velocity magnitude.

From Figure 5, vortices developing in the out flow regions of the 32 crossovers and the dead zones in the branches of the elbow are also clear.

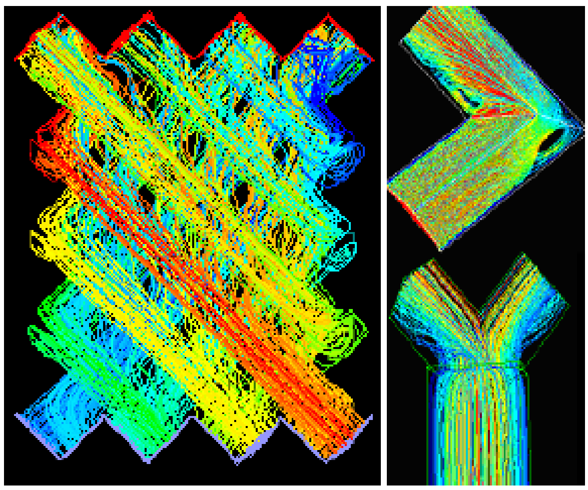

Figure 5. Gas flow path line in the sheet of KATA-PAK and in the elbows

Table 1. Geometrical and surface characteristics of the KATAPAK-S

Packing type	a_p (m^{-1})	Porosity, ε	α (deg)	b (m)	h (m)	Type of surface
KATAPAK-S	128.2	0.622	45	0.0218	0.0115	Gauze

Figure 7 demonstrates the contours of turbulence intensity in the KATAPAK-S sheet. As shown in this figure, percent of turbulence intensity in the junctions is high and the mass transfer flux in these crossovers is higher than other regions.

The contours of static pressure drop at Re=3700 are shown in Figure 6. Dry pressure drop for a sheet can be calculated from this figure. Similarly, the pressure drop for the elbows can be calculated, therefore the total pressure drop is:

$$(\Delta P)_{total} = (\Delta P)_{Sheets} + (\Delta P)_{Elbow-entrance} + (\Delta P)_{Elbow-middle} \quad (12)$$

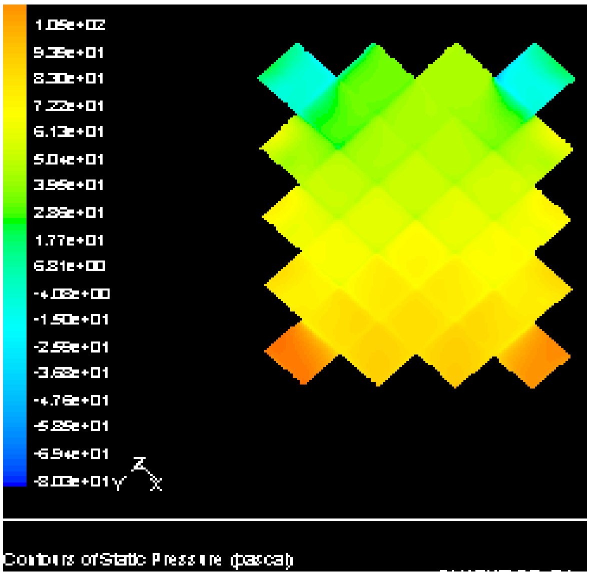

Figure 6. Contours of static pressure at Re=3700

The experimental data for dry pressure drop in KATAPAK-S are those reported by Kolodziej and co-workers [1].

The values of dry pressure drop can also be calculated from the theoretical model mentioned above. From Eq. (6) at F_S=2 m/s (kg/m^3)$^{.5}$ we have:

$$K = 1/\left(1 + 4/a_p D\right) = 0.88 \quad (13)$$

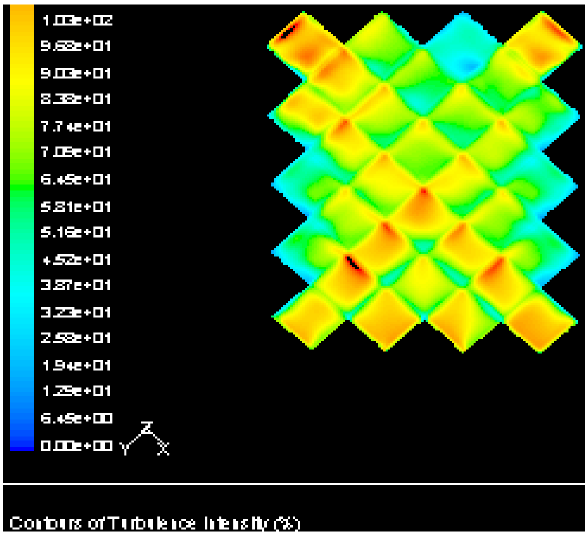

Figure 7. Contours of turbulence intensity (%) at Re=3700

$$d_h = \frac{4\varepsilon K}{a_p} = \frac{4*0.622*0.88}{128.2} = 0.017m \quad (14)$$

$$\mathrm{Re} = \frac{\rho_g.V.d_h}{\mu_g} = 2106 \quad (15)$$

$$\Psi = 2.561*\mathrm{Re}^{-0.171} = 0.69 \quad (16)$$

$$\left(\frac{\Delta P}{H}\right)_{dry} = \Psi*\left(\frac{\rho_g.V^2.a_p}{8\varepsilon^3 K}\right) = 209(pa/m) \quad (17)$$

The pressure drop at F_S=2 m/s(kg/m^3)$^{.5}$ from CFD simulation is 205(pa/m) and from experimental data is 200(pa/m).

For comparison purposes, the data from the theoretical model, and the CFD simulated results are compared with actual experimenttal pressure drop data.

Table 2 and Figure 8 show the results.

In Figure 8, values of total pressure drop $\left(\frac{\Delta P}{H}\right)_{total}$ are plotted against the gas load factor $\left(F_S = V*\sqrt{\rho_g}\right)$.

From this figure it can be seen that CFD model provides excellent agreement between experimental data and the theoretical model.

The average error corresponding to data of Figure 7 is defined by:

$$E(\%) = 100 * \frac{1}{N} \sum \left| \frac{\left(\frac{\Delta P}{H}\right)_{Exp} - \left(\frac{\Delta P}{H}\right)_{CFD}}{\left(\frac{\Delta P}{H}\right)_{Exp}} \right| = 7.2\% \quad (18)$$

Conclusion

The momentum and continuity equations have been solved by a CFD approach to determine the dry pressure drop in KATAPAK-S structures. The low Reynolds $K-\varepsilon$ model was used for the simulation.

The static pressure contours, gas phase path lines and turbulence intensity contours of airflow in the sheet and elbow have been plotted.

The path lines of air flow show the quality of gas distribution in a sheet of KATAPAK-S. Dead zones and vorticity regions can be seen from the path line plot. The flow pattern in the sheet is very complex and the gas phase is in the turbulent regime. The turbulence intensity contours show that the turbulent intensity percent at 32 crossovers is higher than other regions. It has been suggested that the mass transfer flux in the crossovers regions is high.

The contours of static pressure were used to measure gas pressure drop in KATAPAK. Experimental data and theoretical model have been used to validate the CFD model. Results of CFD model showed good agreement with theoretical and experimental data and the average error was 8.51%.

Nomenclature

a	Specific surface area (m^2/m^3)
B	Body force (N/m^3)
b	Channel base (m)
d_h	Hydraulic diameter (m)
E	Average error (%)
F_S	Gas load factor m/s $(kg/m^3)^{.5}$
h	Channel height (m)
K	Wall factor
N	Number of the experiments
P	Pressure (pa)
ΔP	Pressure drop (pa)
Re	Reynolds number
t	Time(s)
U_g	Effective gas velocity (m/s)
V	Superficial gas velocity (m/s)

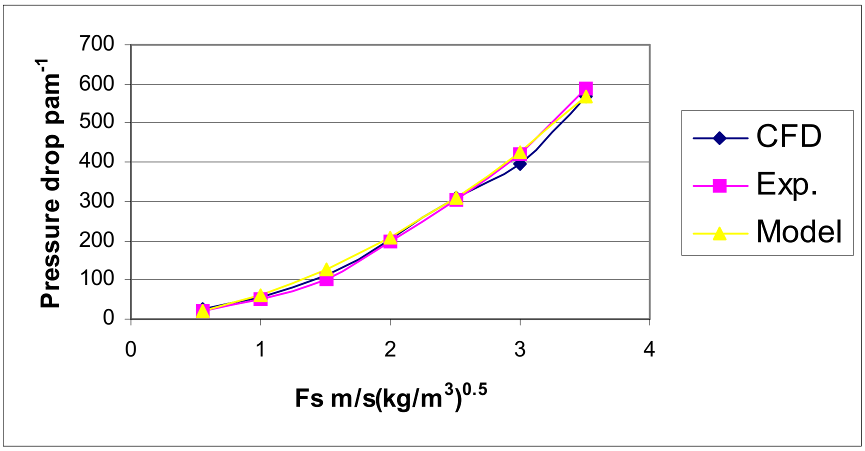

Figure 8. Simulated, experimental and theoretical dry pressure drop versus gas flow factor

Table 2. Results of CFD simulation, theoretical model and experimental pressure drop

F_S m/s(kg/m^3)$^{.5}$	0.55	1	1.5	2	2.5	3	3.5
$\left(\frac{\Delta P}{H}\right)_{sheet(CFD)}$ pa/m	11	33	80	155	235	312	470
$\left(\frac{\Delta P}{H}\right)_{elbow-entrance(CFD)}$ pa/m	2	4	8	10	20	25	29
$\left(\frac{\Delta P}{H}\right)_{elbow-middle(CFD)}$ pa/m	10	20	25	40	55	60	70
$\left(\frac{\Delta P}{H}\right)_{Totalt(CFD)}$ pa/m	23	57	113	205	310	397	569
$\left(\frac{\Delta P}{H}\right)_{Exp.}$ pa/m	20	52	100	200	305	420	590
$\left(\frac{\Delta P}{H}\right)_{Model}$ pa/m	22.5	61	127	209	308	428	567
$E(\%) = \left\lvert \frac{\left(\frac{\Delta P}{H}\right)_{Exp} - \left(\frac{\Delta P}{H}\right)_{CFD}}{\left(\frac{\Delta P}{H}\right)_{Exp}} \right\rvert * 100$	15	9.6	13	2.5	1.6	5.4	3.5

Greek letters

α	Corrugated angle (deg)
ε	Porosity of packing
μ	Gas viscosity (kg/m.s)
ρ	Gas density (kg/m^3)
Ψ	Friction factor

References

1. *Kolodzie*j A., J*aroszy´nski M.*, *Bylica* I.,” *Mass transfer and hydra*ulics for *KATA-PAK-S*”, *Chem. Eng. Processing.* 43, (2004), 457–464.
2. Van Baten J. M. and Krishna R., “Gas and liquid phase mass transfer within KATA-PAK-S structures studied using CFD simulations”, Chem. Eng. Sci.57, (2002), 1531-1536.
3. Van Baten J. M., Ellenberger J. and Krishna R., “Radial and axial dispersion of the liquid phase within KATAPAK-S structures”, Chem. Eng. Sci. 56, (2001), 813-821.
4. Van Baten J. M. and Krishna R., “Liquid phase mass transfer within KATAPAK-S structures studied using CFD simulations”, Catalyst Today.69, (2001), 371-377.

5. Taylor R. and Krishna R., "Modeling reactive distillation", Chem. Eng. Sci. 55, (2000), 5183-5229.
6. Ellenberg J. and Krishna R., "Counter current operation of structured catalytically packed distillation column: pressure drop, hold-up and mixing", Chem. Eng. Sci. 54, (1999), 1339-1345.
7. Fischer L., Buhlmann U. and Melcher R., "Characterization of high performance structured packing", Trans IchemE. 81, (2003), 79-84.
8. Petre C. F., etal. "Pressure drop through structure packings: break down into the contributing mechanisms by CFD modeling", Chem. Eng. Sci. 58, (2003), 163-177.
9. Larachi F., etal. "Tailoring the pressure drop of structured packings through CFD simulations", Chem. Eng. Processing. 42, (2003), 535-541.
10. Olujic Z., "Effect of column diameter on pressure drop of a corrugated sheetstructured packing", Trans IchemE. 72, (1999), 505-510.